COMPARATIVE ANALYSIS OF PROCESS PARAMETERS OF TALC MECHANICAL ACTIVATION IN CENTRIFUGAL AND ATTRITION MILL

Ljubisa ANDRIC[*], Anja TERZIC[**], Zagorka ACIMOVIC-PAVLOVIC[***], Ljubica PAVLOVIC[*], Milan PETROV[*]

[*] Institute for Technology of Nuclear and Other Mineral Raw Materials, Franchet d'Esperey 86, Belgrade, Serbia

[**] Institute for Materials Testing, Vojvode Misica Blv. 43, Belgrade, Serbia, anja.terzic@institutims.rs

[***] University of Belgrade, Faculty of Technology and Metallurgy, Karnegy st. 4, Belgrade, Serbia

Abstract: The efficiency of talc mechanical activation by means of two different mechano-activators - centrifugal and attrition mill is investigated in this study and the comparative analysis of the characteristics of obtained talc powders is presented. A new approach for obtaining high-grade talc concentrate with low Fe_2O_3 content is achieved through effect of mechanical activation of talc accompanied by hydrometallurgical process. The applied mechanical activation process conditions of ultra-centrifugal mill were defined by number of rotor revolutions, sieve mesh size, and current intensity. These operating parameters of the ultra-centrifugal mill were variable. Ultra fine grinding of talc in attrition mill (attritor) was carried out in various time intervals - from 5 to 15 min. The following technological parameters of the mechanical activation were monitored: time of mechanical activation, circumferential rotor speed, capacity of ultra-centrifugal mill, and specific energy consumption. The investigation was based on a kinetic model. The structure and behavior of activated samples were characterized by scanning electron microscopy (SEM), X-ray diffraction (XRD) analysis, and differential thermal analysis (DTA).

Introduction

Talc belongs to the advanced materials which are setting new limits for the industrial standards since their particle size is becoming extremely fine. It is difficult to produce extremely fine particles through plain mechanical milling and furthermore, due to low capacity and high energy consumption the milling is an expensive process (Cho et al., 2006). Talc as a non-metallic raw material is irreplaceable in a large number of industrial applications: ceramics manufacturing (synthesis of the cordierite and

steatite), cast products, paints, rubber, cables, paper, lead, pharmaceutical products, insecticides and herbicides, civil engineering, military industry, etc. The standard way of the talc processing can satisfy only a limited number of the applications. Introduction of the mechanical activation procedure carried out by means of the different types of mechano-activators (centrifugal mill, stirred media mill/attrition mill, jet mill, planetary mill, vibratory mill, mortar mill) can help in overcoming of this problem (Sanchez-Soto et al., 1997, Inoue et al., 1996, Inoue et al., 1999, Lee et al., 2010, Mahmoodian et al., 2013, Neesse et al., 2004, Shinohara et al., 1999, and Perez-Maqueda et al., 2006.).

Centrifugal mill is a variation of the planetary mill in which the mill tube operates in a force field generated by the gyration of the tubes around the common axis. Furthermore, centrifugal mills differ from planetary mills with regard to the ratio of the gyration diameter to the mill tube diameter (G/D), which is less than 1 for centrifugal mills. When G/D becomes very small, i.e. when the mill tube is placed near the center of the rotation, the centrifugal mill begins to resemble a vibration mill. In this sense, the centrifugal mill is a type of vibration mill with increased amplitude of circular vibration (Cho et al., 1999).

Attrition mill (attritor) is applied in the production of fine particles in chemical, pharmaceutical and mineral processing industry, and also, in the process of intensifying of the mineral waste and providing cleaning efficiencies (Schaaff et al. 1999). Attrition mill (stirred-ball mill) enables the production of the submicron particles. In this case, the breakage mechanism can be explained by impact of the operating parameters of attritor mill, such as initial size of particles, ball loading, slurry mass fraction, diameter of grinding media, pin tip velocity and ratio of Young's modulus can influence the Rosin-Rammler equation parameter (Shinohara et al., 1999, and Shrivastava et al., 2011). Particle surfaces are abraded by intense shear and friction stresses between the agitated grinding elements. Attrition grinding can be used as pre-concentration method in talc mineral processing industry. Further removal of carbonates and the separation of talc from chlorite can be obtained by flotation process (Piga et al., 1992). Elongation and smoothness of talc mineral directly influence the increasing of the hydrophobicity or floatability (Yekeler et al., 2004; Yang et al., 2006, and Mahadi et al., 2010).

Mechano-chemical treatment applied on dolomitic talc results in production of ultra fine particles. However, the mechano-chemical treatment might also promote amorphization of talc (Balaz, 2003, Haug et al., 2010, and Tavangarian et al., 2011). Thus, the process of mechanical activation might be considered as pre-treatment to the subsequent hydrometallurgical leaching in order to obtained high-grade talc concentrate with low Fe_2O_3 (Tavangarian et al., 2010 and Zhang et al., 2010).

Material and Methods

Applied material

The sample of the raw talc from "Bela Stena" mine (Serbia) was used in this study. Comminution of raw talc ore was performed by crushing and grinding up to the particle size that could be used as input for the mechanical activation. Particle size distribution, and the results of the chemical and mineralogical analyses performed on talc sample are shown in Table 1.

Table 1. Particle size distribution, chemical and mineralogical composition of raw talc

Class of coarseness (mm)	Mass portion (%)	Undersize (%)	Oversize (%)
-0.589+0.417	6.67	6.67	100.00
-0.417+0.295	13.89	20.57	93.33
-0.295+0.208	19.18	39.74	79.43
-0.208+0.147	16.60	56.35	60.26
-0.147+0.104	15.47	71.82	43.65
-0.104+0.074	10.40	82.22	28.18
-0.074+0.063	3.33	85.55	17.78
-0.063+0.053	3.74	89.28	14.45
-0.053+0.040	3.13	92.41	10.72
-0.040+0.030	2.80	95.21	7.59
-0.030+0.020	2.22	97.43	4.79
-0.020+0.000	2.57	100.00	2.57
Oxides	Content (%)	Talc minerals	Content (%)
SiO_2	37.18		
TiO_2	<0.01	Talc	54.1
Al_2O_3	0.68	Chlorite	8.30
Fe_2O_3	2.6	Quartz	2.20
FeO	3.49	Magnetite	3.40
CaO	3.87	Hematite	0.70
MgO	28.88	Carbonate	29.20
MnO	0.42	Calcite	1.00
Na_2O	0.02	Limonite	0.50
K_2O	0.01	Other	0.60
LoI	22.94		

The basic physico-chemical and mineralogical characteristics of talc were also determined and they are as follows: density $\tau = 2.70$ g/cm^3; humidity $W_1 = 6.00$ %, $W_2 = 0.50$% (after drying); volume density $\varDelta = 1.50$ g/cm^3.

Primary crushing of the raw talc sample was conducted by means of a jaw crusher (output opening sizing 10 mm) working in a closed circle with screen. Afterwards, primary crushed sample was subjected to crushing in the roll crusher (output opening sizing 5 mm). Grinding of the secondary crushed sample was performed in the ceramic-lined ball mill. Ceramic balls were used as grinding media. Ceramic-lined ball mill is working in closed circle with air classifier, which enabled liberation of the minerals presented in Table 1. Afterwards, raw talc ore was subjected to dry micronization in ultra-centrifugal mill and attrition mill (stirring ball mill). The micronization caused partial releasing of the iron mineral, while other minerals (chlorite, quartz, and calcite) were still retained in the sample. The mechanical activation of the talc was conducted by ultra-centrifugal mill and attrition mill.

The activated talc sample was subjected to quantitative characterization. Physical characterization of the ground talc was determined by Coulter Electronics – Coulter Multisizer. The mineralogical composition and microstructural characteristics were determined using X-ray (Philips PW 1710) and scanning electron microscopy (SEM) (Jeol JSM T20) analyses, respectively.

Ultra-centrifugal mill with a peripheral comminution path

The ultra-centrifugal mill with a peripheral comminution path "Retsch ZM-1" was used in this investigation (Gemini BV, Netherlands). The ultra-centrifugal mill "Retsch ZM-1" is supplied with rotor made of high alloyed steel. A number of rotor revolutions can be adjusted (10.000 or 20.000 rpm). Diameter of the rotor (D) was 100 mm. The ring sieve of variable mesh size is static element of the ultra-centrifugal mill also made of high alloyed steel. The two elements together make a reacting system for transfer of energy from a device to a dispersive phase-mechanical activated product.

Ultra-centrifugal mill with a vibrating adder can operate discontinuously or continuously. Mechanical reduction of coarse particles was performed by means of a dynamic counter-balancing of material between working element (rotor) and ring sieve. Rotor cogs are shaped as three-sided prisms placed on a basis, while one its side is turned towards the sieve. This shape of cogs enables streaming of air and fluidized dispersed material.

The tolerance between rotor cogs and ring sieve is 1 mm. It creates a ring volume of $V = 4.74$ cm^3 during the mechanical activation. Due to a high rotor speed and strong centrifugal force, this space is permeable in one direction only - towards the sieve. A principle of dynamic counterbalancing is particle movement from rotor to the sieve and vice versa in the ring zone. Finally, material leaves this zone only when the particle size becomes smaller from the mesh size. Dry mechanical activation of talc in four series of experiments was carried out. The experiments were based on a grinding

kinetic model. It means that achieved results can be described by the Rosin-Ramler-Sperling graph-exponential function and equation as well.

Mathematical interpretation

By applying the Rosin-Ramler-Sperling graph, average particle size (d') dependency on circumferential rotor speed (v) of ultra-centrifugal mill with a peripheral comminution path may be formed. The layout of this dependency is presented in Fig. 1 (Senna, 2010).
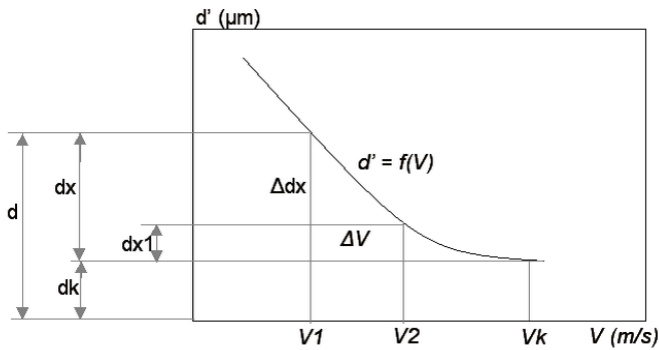
Fig. 1. Average grain size (d') vs. circumferential rotor speed (v)

The slope or position of the curves could be changed. Their changes depend on operational conditions of ultra-centrifugal mill. The experimental results may be described by functional dependence of average grain size (d') vs. circumferential rotor speed (v).

With the increase of circumferential rotor speed (v) the average grain size (d') abruptly decreases. At the same time, this tendency is slowing down towards the final value ($d' > 0$), and vice versa. This is the common characteristic for all curves $d'_i = f_i(v)$ (Ocepek, 1976, Heinicke, 1984, Yvon et al., 2005, and Andric et al., 2005).

According to what was said this phenomenon may be expressed by an exponential equation:

$$y = y_0 \cdot \exp^{-kt} \qquad (1)$$

where: k – constant which depends on the experimental conditions; and y_0 – starting value of (y) that is analogue to the equation $R = R_0 \exp^{-kt}$.

The characteristic phenomenon could be significant for the curve $d' = f(v)$. It could be increased when the value of parameter d' inclines toward definite value d'_k. In this case, the value d'_k is equivalent with the value v'_k. According to this, the value

of d' is split into two portions: a constant portion d'_k and variable portion d'_x. It can be seen on Fig.1.

Based on the analysis of the diagram given in Fig. 1. the following equation can be deducted:

$$d' = d'_x + d'_k .$$ (2)

The dependence between the influential parameter v could be determined. Namely, if the circumferential speed of rotor v is increased up to the value v_1, for a slight value change Δv, it means the value d'_x will automatically be decreased to the d'_{x1} value, also for a slight value change of $\Delta d'_x$.

This must be proportionally equivalent to the exponential equation (Eq. 1). By analogy to the equation $R = R_0 \exp^{-kt}$ the next relation $\Delta d'_k / \Delta v$ is equivalent to d'_x. The following equation is including the factor of proportionality k:

$$\frac{dd'_k}{\Delta v} = -kd' .$$ (3)

Solving differential equation (Eq. 3), the next equation is obtained:

$$\frac{dd'_k}{dv} dv = -kd'_k \Rightarrow \frac{dd'_k}{d'_k} = -kdv .$$ (4)

Further integrating,

$$\int dd'_k / d'_k = \int -kdv \Rightarrow \ln d'_k - \ln d_0 = -kv + kv_k \Rightarrow \ln d'_k / d'_0 = -k(v - v_k),$$ (5)

the equation in the following form is obtained:

$$d'_x = d'_0 \exp^{-k(v - v_k)} .$$ (6)

Using equations (2) and (6) the next equation is obtained:

$$d' = d'_x + d'_k = d'_k + d'_0 e^{-k(v - v_k)} .$$ (7)

In all series of mechanical activation experiments, the following operational parameters of ultra-centrifugal mill were variable: number of rotor revolutions (rpm), screen mesh size (μm) and current intensity (A). Also, dry mechanical activation experiments were preformed under the following conditions: time of mechanical activation, t (min); circumferential rotor speed, v (m/s); capacity of ultra-centrifugal mill, Q (kg/h) and specific energy consumption, W_e (kWh/t).

Achieved experimental results of mechanical activation were observed trough the following parameters: d_1 and d_2 – the mesh sizes of the used screens, μm; R_1 and R_2 –

cumulative oversize, %; d' – parameter which depends on particle size distribution of the sample. It characterizes sample coarseness at the same time represents the measure of the mesh size for oversize cumulative $R = 36.79\%$; n – parameter which depends on particle size distribution of the sample; d_{95} – sieve mesh size that is appropriate to 95% cumulative undersize of the micronized product, μm; S_t – calculated-theoretical specific surface, (m^2/kg); and S_r – real specific surface, m^2/kg.

Attrition mill (Attritor)

In this investigation attrition mill type RSG.INC-ufg-10 (RSG Inc, located in Sylacauga, Alabama USA) was used (www.airclassify.com). High-energy attrition mill ("attritor" or "stirred ball mill") is one of the most efficient devices for fine and ultrafine dry micronization of material. The key of its efficiency is in possibility to input material directly into dry micronization section where no rotation or vibration of the working elements exists. The grinding media is formed of small balls made of stainless chromium-nickel steel, glass, or various ceramic materials of high purity. In this study, chromium-nickel steel balls in diameter range of 0.5–5 mm were used. The attrition mill contains internally agitated media. The attritor can be used for dry grinding and for wet grinding, but in this laboratory testing the attritor for dry grinding was used. The power input is directly used for driving of agitating media which is the key of grinding efficiency and the great advantage compared to other mechano-activators.

The operation of attritor is simple and effective. The material is placed in the stationary grinding chamber of attritor with the grinding media. The material and media are agitated by a rotating central shaft with arms. Particle size reductions and homogeneous particle dispersion with very little wear on the chamber walls were performing by impact and shearing action. The configuration of the attritor arms enables a constant motion of the material and grinding media around the grinding chamber. The area of the greatest media agitation is located approximately on two-thirds of the radius from the center shaft. In machine production, the movement is augmented by adding a pumping, circulation system. Grinding does not take place against the tank walls. This is great advantage, because it enables little wear on the walls, at the same time, leading to longer service life of the vessel. For this reason, the vessel walls can be made thinner and by providing enhanced head transfer and greater temperature control.

The following equation can be used to relate grinding time to media diameter and agitator speed:

$$t = KD^2 / \sqrt{N} \tag{8}$$

where t is grinding time for achieving a certain median particle size; K – constant, depends on processed material, type of media and the model of used attritor; D – grinding media diameter; N – number of shaft revolution, rpm.

From Eq. 8 can be seen that the total grinding time is directly proportional to the media, or square of ball diameter, at the same time, inversely proportional to the square root of the number of shaft revolution. From Eq. 8 it can be concluded that by increasing media size, the grinding time will be increased and vice versa.

Hydrometallurgical leaching

Mechanically activated talc, from both devices, was subjected to leaching by hydrochloric acid (15% wt). Leaching was performed at a constant temperature ($T = 80\ °C$), in three-neck bottle for time period of 3.5 hours. During the process, calcite (green) was separated in bottom layer, at the same time talc concentrate (white) was separated in upper layer. Carbon dioxide (CO_2) was produced during the leaching process, carrying the fine talc particles to concentrate while lighter than chlorite particles remained at the bottom. In addition talc concentrate in warm condition was rinsed by water, then filtered and dried. The same process was applied to chlorite and intermediate product (talc-chlorite) and a final tailing were produced.

Results and Discussion

Results of mechanical activation of talc by means of ultra-centrifugal mill

Comprehensive experimental results of mechanical activation kinetics are shown in Tables 2 and 3.

The results for all sieve mash sizes (80, 120, 200, 500 μm) at nominal number of rotor revolution transition $n_0 = 20000$ rpm and/or $n_0 = 10000$ rpm were presented. It can be seen that with increasing of the mechano-activator load, the current intensity was increased from 1.20 A to 4.00 A. The following experimental results were found: technological parameters of mechanical activation were changing with the increasing of the mechano-activator load; The reduction of mechanical activation time t directly effected increasing of the mechanoactivator capacity Q; The values of parameter d_{95}, which defines a fineness of mechanical activation, were increased.

The increased values of parameter d_{95} indicated that the increasing of coarseness of the talc sample. It means that the value of parameter d' was increasing, while the value of parameter v was decreasing. The reduction of parameters S_t, S_r and W_e were observed as well. Specific surface and specific energy consumption were decreased.

Table 2. Parameters of mechano-activator and of mechanical activation procedure

Series number	Experim. Seq. no.	Parameters of ultra-centrifugal mechano-activator				Technological parameters of mechanical activation			
		RPM	Actual number of RPM	Sieve size (μm)	Current intensity (A)	Duration (min)	Speed (m/s)	Mechanical capacity (kg/h)	Energy consumption (kWh/t)
I	1		14.62		1.40	15	75.36	0.10	290.96
	2	10000	10.72	80	2.30	7	55.26	0.22	220.22
	3		9.46		3.00	5	48.78	0.31	165.2
	4		8.22		3.75	3	42.37	0.52	106.25
	5		23.89		2.10	13	123.11	0.12	235.94
	6	20000	22.65	80	2.30	6	116.74	0.26	220.22
	7		21.02		2.80	4	108.33	0.39	180.92
	8		17.25		3.50	2	88.88	0.78	125.9
II	1		14.62		1.40	8	75.36	0.19	290.96
	2	10000	13.65	120	1.60	5	70.34	0.31	275.24
	3		10.01		2.70	2	51.58	0.78	188.78
	4		8.36		3.50	1	43.09	1.55	125.9
	5		22.65		2.20	6	116.74	0.26	228.08
	6	20000	20.02	120	2.50	3	103.17	0.52	204.5
	7		18.54		3.00	1.5	95.55	1.03	165.2
	8		15.98		4.00	0.8	82.35	1.94	86.6
III	1		14.62		1.40	4	75.36	0.39	290.96
	2	10000	11.94	200	1.90	1	61.55	1.55	251.66
	3		9.84		2.80	0.5	50.7	3.10	180.92
	4		8.09		3.80	0.2	41.67	7.75	102.32
	5		23.33		2.20	3	120.26	0.52	228.08
	6	20000	21.02	200	2.60	0,6	108.33	2.58	196.64
	7		18.93		3.00	0.1	97.57	15.50	165.2
	8		16.37		4.00	0.08	84.37	19.38	86.6
IV	1		14.62		1.20	3	75.36	0.52	306.68
	2	10000	11.94	500	2.00	0.5	61.55	3.10	243.8
	3		10.01		2.80	0.1	51.58	15.50	180.92
	4		9.46		3.20	0.06	48.78	25.83	149.48
	5		22.65		2.20	2	116.74	0.78	228.08
	6	20000	21,02	500	2.40	0.7	108.33	2.21	212.36
	7		20.02		2.80	0.06	103.17	25.83	180.92
	8		18.54		3.20	0.02	95.55	77.50	149.48

Table 3. Mechanical activation product parameters

Series number	Exper. sequence number	RPM	d_1 (µm)	d_2 (µm)	R_1 (%)	R_2 (%)	$d^{'}$ (µm)	n	d_{95} (µm)	S_t (m²/kg)	S_r (m²/kg)
I	1	10000	1	8	73	6	2.96	1.05	8.10	3839.45	4607.34
	2		1	8	78	4	3.1	1.89	7.30	2405.46	2886.56
	3		1	8	80	5	3.3	1.25	7.70	2170.52	2604.62
	4		1	8	86	4	3.4	1.47	7.40	1445.63	1734.76
	5	20000	1	8	77	10	3.6	1.05	9.80	3261.76	3914.12
	6		1	8	82	8	3.8	1.22	8.90	2019.20	2423.04
	7		1	8	85	7	3.9	1.34	8.40	1595.13	1914.16
	8		1	8	88	7	4.13	1.46	8.40	1294.90	1553.88
II	1	10000	1	8	85	5	3.7	1.40	7.70	1556.81	1868.17
	2		1	8	87	7	4	1.42	8.40	1387.53	1665.04
	3		1	8	80	14	4.2	1.05	11.40	2804.05	3364.86
	4		1	8	91	16	5.2	1.43	10.90	1053.44	1264.13
	5	20000	3	10	73	11	6.1	1.62	11.70	739.16	886.99
	6		3	10	79	16	7	1.70	13.00	604.61	725.54
	7		3	10	84	16	7.3	1.95	12.60	497.97	597.57
	8		3	10	85	17	7.5	1.98	12.70	480.35	576.42
III	1	10000	1	8	88	16	5	1.28	11.30	1368.19	1641.83
	2		1	10	89	18	6.3	1.17	15.50	1350.86	1621.04
	3		1	10	94	26	8	1.34	17.60	777.36	932.83
	4		1	15	93	21	10.1	1.13	25.60	912.33	1094.79
	5	20000	1	8	89	11	4.6	1.41	9.60	1224.65	1469.58
	6		1	10	88	10	5.1	1.26	11.90	1384.73	1661.68
	7		1	10	89	16	6	1.20	14.50	1326.33	1591.59
	8		1	15	90	16	8.4	1.05	22.90	1356.94	1628.32
IV	1	10000	1	10	85	19	6	1.01	17.10	2196.60	2635.92
	2		2	10	80	22	7.1	1.19	17.10	1149.66	1379.59
	3		2	12	92	17	8.6	1.71	15.90	492.89	591.46
	4		1	15	92	17	9	1.13	22.90	1033.73	1240.48
	5	20000	2	13	92	28	11	1.46	22.70	483.11	579.74
	6		2	15	92	27	12.3	1.37	26.60	484.46	581.35
	7		5	17	89	28	15	1.95	25.70	243.11	291.73
	8		5	19	91	29	17	1.93	29.30	217.41	260.89

Mathematical interpretation of talc mechanical activation by mean of ultra-centrifugal mill

The experimental results of mechanical activation of mica could be explained by parameter d'. Parameter d' provides the best approximations of experimental measurements and is presented by the equation

$$d' = d'_k + d'_0 \cdot \exp^{-k \cdot (v - v_k)}. \tag{9}$$

Inserting the experimental values from Tables 2 and 3 in (Eq. 9), the charts of average grain size vs. circumferential rotary speed $d' = f(v)$ for all sieves mesh sizes were obtained. The charts of dependency of average grain size d' on circumferential rotary speed are presented in Figs. 3-6, respectively.
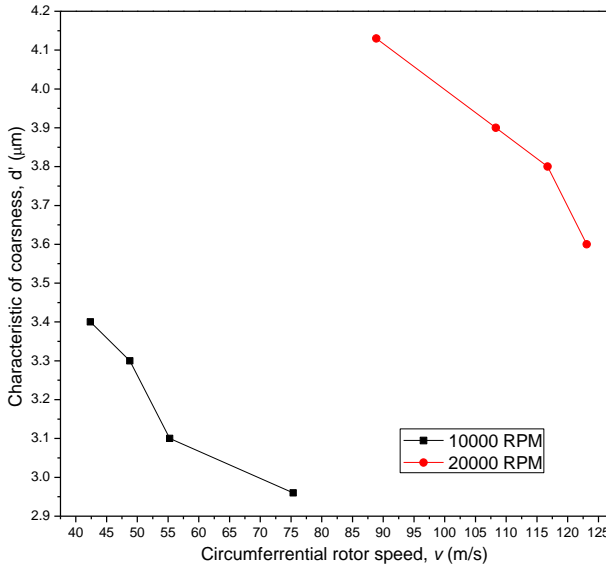
Fig. 2. Average grain size d' of mechanically activated talc vs. circumferential rotor speed v of ultra-centrifugal mill for sieve mesh size 80 μm

Experimental investigation of mechanical activation of talc in the ultra-centrifugal mill showed that this method did not provide good quality talc with a low iron content ($Fe_2O_3 = 1.00–1.50\%$).
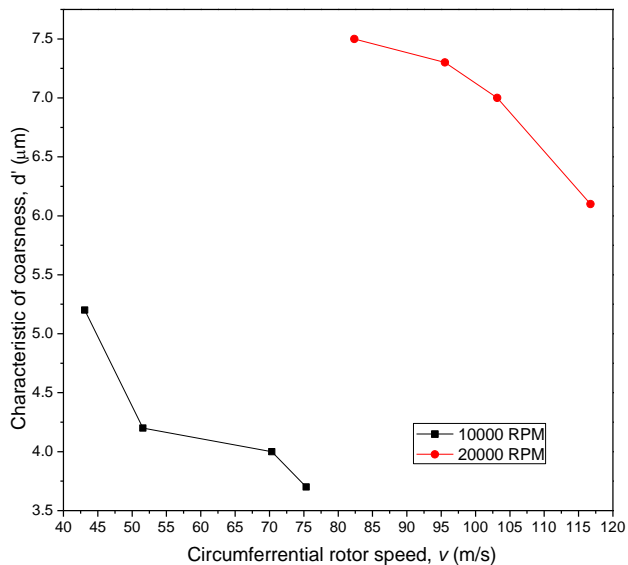
Fig. 3. Average grain size d' of mechanically activated talc vs. circumferential rotor speed v of ultra-centrifugal mill for sieve mesh size 120 μm
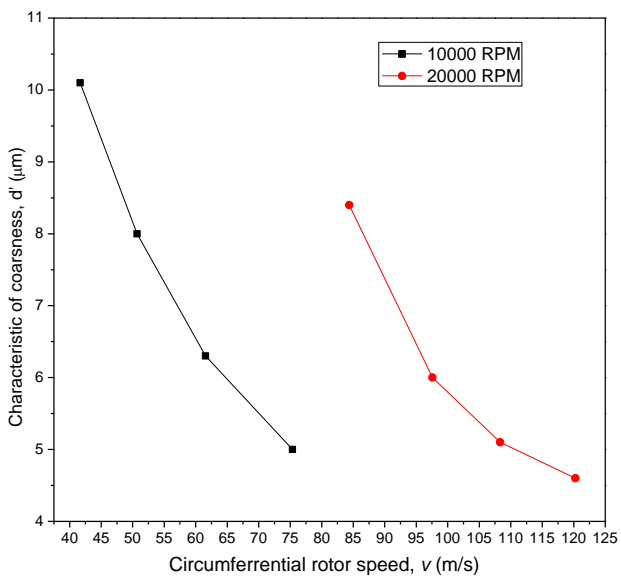
Fig. 4. Average grain size d' of mechanically activated talc vs. circumferential rotor speed v of ultra-centrifugal mill for sieve mesh size 200 μm
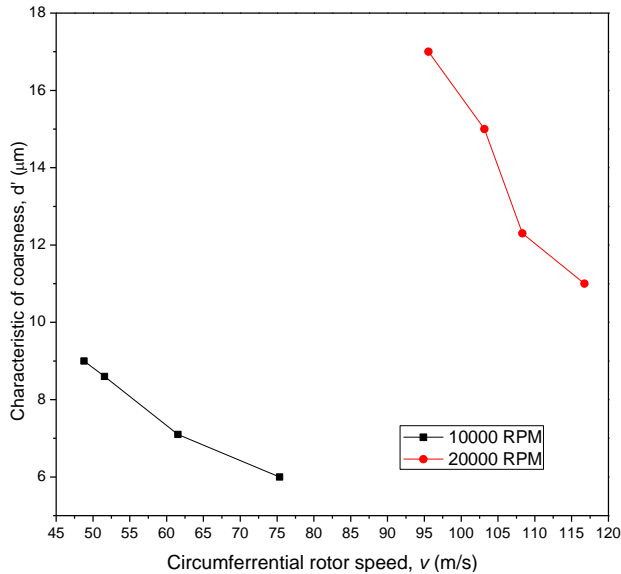
Fig. 5. Average grain size d' of mechanically activated talc vs. circumferential rotor speed v of ultra-centrifugal mill for sieve mesh size 500 μm

Achieved results of mechanical activation of talc by means of attrition mill

Fine and ultra fine milling of talc in attrition mill (attritor) were carried out at various time periods from 5 to 15 min. At the same time, the data of talc grinding in vibratory and conventional ball mill for milling time periods from 8 to 40 min were used for comparison and detailed assessments. Experimental data are listed in Table 4.

Operating the attrition mill is simple. Its efficiency is based on ceramic materials milling in the submicron zone, while other mills (conventional and some types of vibratory mills) cannot efficiently operate in this zone to produce sub micro particles. Table 4 shows that for specific energy consumption of 150 kWh/megagram, the average size of particles obtained by attrition mill is decreasing, i.e. the particles are finer. For specific energy consumption above 200 kWh/t, attrition mill continues ultrafine grinding in sub micro zone. Other mills have either longer grinding time or higher (or equal) specific energy consumption. However, they produce particles with higher average size than attrition mill. This points out to the fact that attritor has shorter milling time, it produces material with lower average particle size, and thus, it is more efficient than other mills used in comparative analysis.

Figure 6 shows the relative ultra fine grinding effectiveness of talc by attrition, vibratory and conventional ball mills. It can be seen that the curve for the vibratory ball mill is on the top, two middle curves are describing ultra fine talc grinding effectiveness in conventional ball mill, and the bottom curve is describing ultra fine talc grinding effectiveness in attritor.

L. Andric, A. Terzic, Z. Acimovic-Pavlovic, L. Pavlovic, M. Petrov

Table 4. Milling efficiency of attritional mill (Attritor-stirred ball mill)

Type of mill	Milling time - t, min	Specific energy consumption - W_e, kWh/Mg	Average particle Size - d, μm
Conventional ball mill (wet milling)	27.50	361.54	2.30
	25.00	176.92	3.60
	17.00	92.33	4.80
	11.00	61.54	5.80
Conventional ball mill (dry milling)	15.00	423.09	1.80
	10.00	211.62	2.20
	8.00	130.76	3.00
Vibratory mill with balls	40.00	361.54	3.80
	23.00	176.92	4.50
	20.00	50.00	8.00
Attritional mill	15.00	423.09	1.00
	13.00	284.74	1.30
	10.00	176.92	1.60
	8.00	146.29	2.00
	6.00	61.54	2.80
	5.00	30.76	3.00
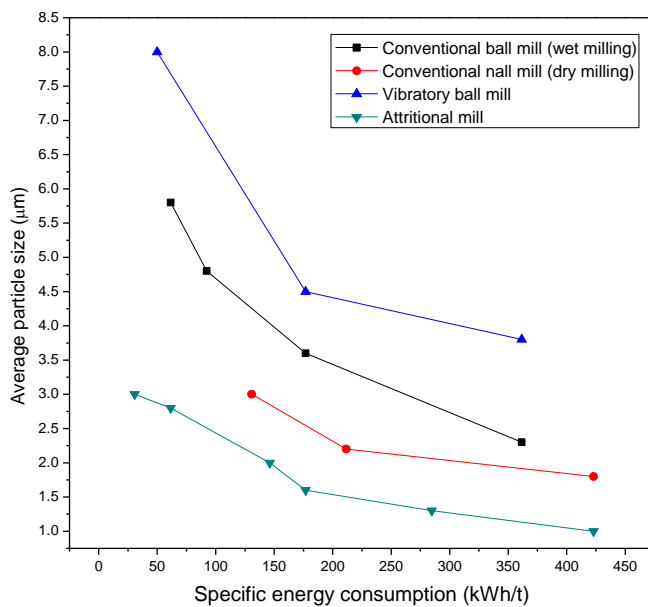
Fig. 6. The mean particle size vs. specific energy input in various mills

For a specific energy input of approximately 100 kWh/Mg the mean particle diameter produced by the attritor is approximately 50% smaller than the mean particle diameter obtained with the conventional ball mill. At the same time, the mean particle diameter obtained by attritor is about 33% lesser than mean particle diameter obtained by vibratory ball mill. At a specific energy input above 200 kWh/Mg, the attritor continued to grind to the submicron range, while other machines could not longer efficiently produce small submicron particles. Therefore, the time required for grinding of submicron particles is much shorter for the attritor.

During dry milling of talc in attritor, iron minerals have been released, while other minerals such as chlorite, quartz and calcite were still retained in the talc sample. It was confirmed by microscopic examination. It indicated that this method is not enable to provide good quality talc with low iron content ($Fe_2O_3 = 1.00–1.50\%$).

Achieved results of mechanical activation of talc in ultra- centrifugal and attrition mill did not provide good quality talc with low iron content ($Fe_2O_3 = 1.00–1.50\ \%$). For this reason hydrometallurgical method was applied.

Hydrometallurgical leaching of mechanically activated talc

Mechanically activated talc, from both devices, was subjected to leaching by hydrochloric acid (15% wt). Results of dry mechanically activated talc which underwent hydrometallurgical leaching were confirmed by physico-chemical, mineralogical, X-ray and DTA data, which are presented in Tables 5 and 6 and Figs. 7–10.

Table 5. Particle size distribution of talc ($n = 1.34$; $d' = 3.9$; $d_{95} = 8.4$; $St = 1595.13$ m^2/kg)

Class of coarseness (µm)	Mass portion (%)	Undersize (%)	Oversize (%)
-10+9	3	3	100.00
-9+8	4	7	97
-8+5	15	22	93
-5+3	34	56	78
-3+2	14	70	44
-2+1	15	85	30
-1+0	15	100.00	15
Total	100.00		

Table 6. Chemical composition of talc concentrate, intermediate product and tailing

Product	Component and content				
	Mass portion (%)	MgO (%)	Fe$_2$O$_3$ (%)	LoI (%)	Mineral
Talc concentrate	75.90	28.30	1.15	5.00	pure talc
Intermediate product	15.77	12.94	5.83	6.90	talc chlorite
Tailing	8.33	14.57	10.00	9.75	chlorite
Total	100.00	24.22	2.80	5.84	-

In order to explain the influence of mechano-activation on the structure and characteristics of talc and to confirm results obtained during mechanical activation, specific analyses were performed before and after activation procedure including differential thermal analysis (DTA); X-ray powder diffraction analysis (XRD) and scanning electron microscopy (SEM).

The DTA curve for talc is presented in Fig. 7. The peaks appearing at 390 °C and 850 °C are exothermic. Talc is relatively thermally stable up to 850 °C after which the endothermic effect was noticed. The endothermic effect reached its peak at 967 °C. This effect could be explained by the loss of structural water by recrystallization into enstatite ($MgSiO_3$) (Andric et al., 2005). Melting of the talc samples is not recorded. There were not significant changes of the DTA curve of the mechanically activated talc sample in comparison with the DTA curve recorded before activation treatment. Namely, mechanical activation procedure does not influence shifting of the endothermic and exothermic peaks on talc DTA curve. Also it does not initiate decreasing of the melting point for talc.
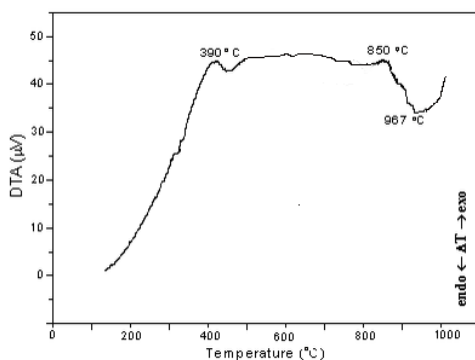
Fig. 7. DTA diagram of mechanically activated talc

Mineralogical phase changes as well as variations in crystallinity occurring in the talc samples were monitored by means of the XRD analysis. In Figs 8 and 9 the diffractograms of talc sample before and after mechanical activation are given. It was noticed that changes in the crystal structure of talc appeared within 30 minutes of the mechanical activation process. Mechanical reduction of the original particles of investigated mineral appears to have reached a limit at 30 minutes grinding time and longer grinding times might produce opposite effect, that is an increase in the particle size.

It can be concluded that mechanical activation influences the crystal structure of talc, i.e. level of crystallinity is decreasing with the increasing mechano-activation time. The mechanical activation makes the structure disordered and generates crystal lattice defects or other meta-stable forms. The mechano-activation treatment can promote the amorphization of treated material, noticeable change of the micro-structure, size and shape of particles etc.
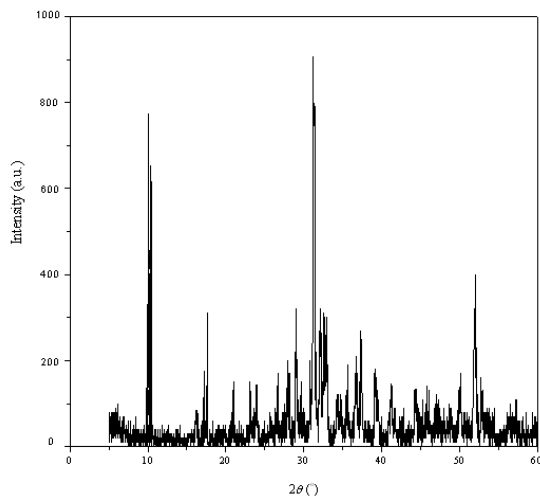
Fig. 8. Diffraction peak values and intensities of original talc sample (before activation)
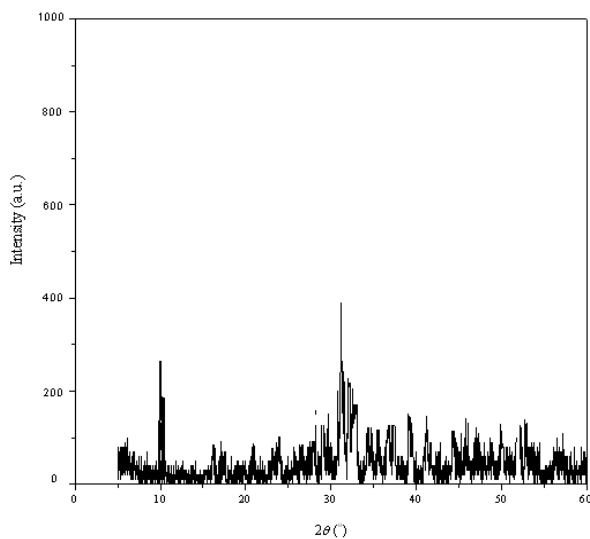
Fig. 9. Diffraction peak values and intensities of talc sample after mechanical activation

The original talc particles are rounded, slightly elongated and the dimensions of the original talc particles vary significantly. The SEM microphotograph of talc sample after mechanical-activation, which is given in Fig. 10., shows that the talc particles gained rather angular shape. The talc particles possess a semi-layered structure while their size is reduced and rather uniform.
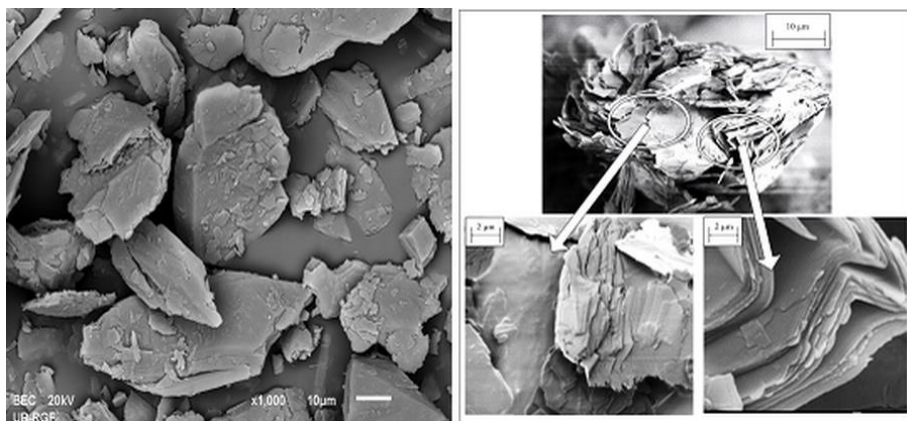
Fig.10. SEM microphotograph of talc after mechanical activation

Conclusion

Good liberation of raw talc ore was achieved by means of mechano-activation performed by means of ultra-centrifugal and attrition mills. The obtained talc concentrate had homogenous particle size distribution, low content of Fe_2O_3, and 5% loss on ignition. The X-ray analysis showed presence of 98% of pure talc accompanied only by negligible amounts of chlorite and quartz. However, the hydrometallurgical leaching is adequate additional procedure which could successfully elevate the iron content and improve the overall quality of the activated talc product.

Investigation of talc mechanical activation in both ultra-centrifugal and attrition mills, pointed out to the fact that the characteristics of the dry activated product directly depend on the values of technical-technological parameters of the activation procedure. The rate of the mechanical activation in the ultra-centrifugal mill was increasing with the increase of the amplification of mill load and of rotor revolutions. The rate of the mechanical activation reached the highest level at the nominal load of ultra-centrifugal mill, i.e. the best performance was achieved for a full ultra-centrifugal mill. It was concluded that the attrition mill was suitable for specific energy consumptions above 200 kWh/Mg, because the attritional mill continued ultra fine grinding in the submicron zone. This, furthermore, points out to a relatively short milling time which is a huge advantage of attrition mill in comparison to other grinding devices.

The DTA analysis showed that activation did not cause shifting of the melting point of the activated talc in comparison with non-activated product, meaning that the activated talc would not melt when applied in a high temperature material. The X-ray analysis of the non-activated and activated talc samples confirmed that mechanical activation contributes to the decreasing of its crystallinity and transformation in the amorphous state. Additionally, the SEM analysis showed that the activated talc particles were reduced in size and became more uniform, which facilitate better

packing of the filler particles in a material. A better 'packing' of the components in the material structure influences the increase of the material strength.

Acknowledgements

References

ANDRIC, LJ, MILOŠEVIC, V., PETROV, M., MIHAJLOVIC, S., 2005, *Operating Technique of Mills in the process of Micronization Milling of Alumina*, J. Mining and Metallurgy 41A, 27–43.

BALAZ P. 2003, *Mechanical activation in hydrometallurgy*, Int. J. Miner. Process. 72, 341– 354.

CHO H., LEE H., LEE Y., 2006, *Some breakage characteristics of ultra-fine wet grinding with a centrifugal mill*, Inter. J. of Min. Process. 78, 250–261.

HAUG T.A., KLEIV R.A., MUNZ I.A., 2010, *Investigating dissolution of mechanically activated olivine for carbonation purposes,* Applied Geochem. 25, 1547–1563.

HEINICKE G., 1984, *Tribochemistry*, first ed., Academie-Verlag, Berlin.

INOUE T., OKAYA K., 1996, *Grinding mechanism of centrifugal mills – a simulation study based on the discrete element method*, Int. J. Miner. Process. 44–45, 425–435.

INOUE T., OKAYA K., OWADA S., HOMMA T, 2010, *Development of a centrifugal mill a chain of simulation, equipment design and model validation*, Powder Technology. 105, 342–350

LEE H., CHO H., KWON J., 2010, *Using the discrete element method to analyze the breakage rate in a centrifugal/vibration mill,* Powder Technology 198, 364–372

MAHADI M.I., PALANIANDY S., 2010, *Mechanochemical effect of dolomitic talc during fine grinding process in mortar grinder,* Int. J. Miner. Process. 94,172–179.

MAHMOODIAN, R., HASSAN, M.A., RAHBARI, R.G., YAHYA, R., HAMDI, M., 2013, *A novel fabrication method for TiC–Al2O3–Fe functional material under centrifugal acceleration,* Composites: Part B 50,187–192.

NEESSE TH., SCHAAFF F., TIEFEL H., 2004, *High performance attrition in stirred mills*, Minerals Engineering 17, 1163–1167.

OCEPEK D., 1976, *Mehanska procesna tehnika*, first ed. D.D.U., Ljubljana (in Serbian).

PEREZ-MAQUEDA L.A., DURAN A., PEREZ-RODRIGUEZ J.L, 2006, *Preparation of submicron talc particles by sonication*, Appl. Clay Sci. 28, 245–255.

PIGA L., MARRUZZO G., 1992, *Preconcentration of Italian talc by magnetic separation and attrition*, Int. J. of Min. Process. 35, 291–297.

SANCHEZ-SOTO P.J., WIEWIORA A., AVILES M.A., JUSTO A., PEREZ-MAQUEDA L.A., PEREZ-RODRIGUEZ J.L., BYLINA P., 1997, *Talc from Puebla de Lillo, Spain. II. Effect of dry grinding on particle size and shape*, App. Clay Sci. 12, 297–312.

SCHAAFF F, SCHNEIDER M., NEEGE TH., 1999, *Intensifying the attrition of mineral waste in stirrer mills*, Int. J. Miner. Process. 74S, S291–S298.

SENNA M., 2010, *Finest grinding and mechanical activation for advanced materials*, 7th European Symposium on Comminution, Ljubljana, 21–37.

SHINOHARA K., GOLMAN B., UCHIYAMA T., OTANI M., 1999, *Fine-grinding characteristics of hard materials by attrition mill,* Powder Technology 103, 292–296.

SHRIVASTAVA A., SAKTHIVEL S., PITCHUMANI B., RATHORE A.S., 2011, *A statistical approach for estimation of significant variables in wet attrition milling*, Powder Tech. 211, 46–53.

TAVANGARIAN F., EMADI R., SHAFYEI A., 2010, *Influence of mechanical activation and thermal treatment time on nanoparticle forsterite formation mechanism*, Powder Techn. 198, 412–416.

TAVANGARIAN F., EMADI R., 2011, *Effects of mechanical activation and chlorine ion on nanoparticle forsterite formation,* Materials Letters 65,126–129.

www.geminibv.nl/labware/retsch-zm1-grinder, Gemini BV, Netherlands

www.airclassify.com/

YANG H., DU C., HU Y., JIN S., YANG W., TANG A., AVVAKUMOV E.G., 2006, *Preparation of porous material from talc by mechanochemical treatment and subsequent leaching*, App. Clay Sci. 31 (2006) 290–297.

YEKELER M., ULUSOY U., HICYILMAZ C., 2004, *Effect of particle shape and roughness of talc mineral ground by different mills on the wettability and floatability*, Powder Tech. 140, 68–78.

YVON J., VILLIERAS F., MICHOT L., 2005, *Effect of Different Dry Grinding Procedures on the Immersion Heat of Talc and Chlorite*, J. Mining and Metallurgy 41A, 1–9.

ZHANG Y, LI X., PAN L., WEI Y, LIANG X, 2010, *Effect of mechanical activation on the kinetics of extracting indium from indium-bearing zinc ferrite*, Hydrometallurgy 102, 95–100.